Article ID: 1007-4627(2016) 01-0025-05

Dileptons and Photons Production in Ultrarelativistic Heavy Ion Collisions from the Color Glass Condensate

YU Gongming[1], YANG Haitao[2], LI Yunde[1]

(*1. Department of physics, Yunnan University, Kunming 650091, China;*
2. School of physics and electronic information engineering, Zhaotong University, Zhaotong 657000, Yunnan, China)

Abstract: We investigate inclusive dileptons and photons production in relativistic heavy ion collisions based on the idea of gluon saturation in the color glass condensate (CGC) framework. In the gluon saturation region, the dominant mechanism for low-$p_{\rm T}$ dileptons and photons production in the perturbative approach (the $k_{\rm T}$-factorization approach) is gluon-gluon interaction. At Relativistic Heavy Ion Collider (RHIC) and Large Hadron Collider (LHC) energies, the value of saturation momentum becomes larger than the Quantum Chromodynamics (QCD) confinement scale $\Lambda_{\rm QCD}$ for relativistic heavy ion collisions, which implies that $\alpha_{\rm s} \ll 1$. In this state, the gluon density for proton and nucleus with transverse momentum less than the saturation momentum $Q_{\rm s}$ will reach a high value, and the invariant cross-section for dileptons and direct photons is further enhanced by saturation effects. The numerical results indicate that the production of low-$p_{\rm T}$ dileptons and photons from the color glass condensate becomes prominent in pp, pA, and AA collisions at RHIC and LHC energies.

Key words: dilepton; photon; color glass condensate; heavy ion collision

CLC number: O571.6 **Document code:** A **DOI:** 10.11804/NuclPhysRev.33.01.025

1 Introduction

In relativistic heavy ion collisions, the perturbative Quantum Chromodynamics (pQCD) predicts a high gluon density which are expected to saturate at a scale $Q_{\rm s}$ forming a color glass condensate (CGC)[1]. In this state, the parton density with transverse momentum less than the saturation momentum $Q_{\rm s}$ will reach a high value. Since the Lorentz contraction of the nuclear parton density in the probe rest frame, the saturation momentum $Q_{\rm s}$ has an A and x dependence, where A is the numbers of nucleon. The gluon dynamics in the the saturation regime is non-perturbative as is typical of strongly correlated systems. In recent years, there has been much work done to investigate the properties of the CGC in deep inelastic electron-proton and electron-nucleus scattering, as well as proton-proton, proton-nucleus, deuteron-nucleus and nucleus-nucleus collisions, such as Dokshitzer-Gribov-Lipatov-Altarelli-Parisi (DGLAP) equation[2–4], Balitsky-Kovchegov non-linear equation[5–6], Jalilian-Marian, Iancu, McLerran, Weigert, Leonidov and Kovner (JIMWLK) renormalization group equation[7–12], Iancu-Mueller factorization[13–15] and McLerran-Venugopalan (MV) model[16–18]. Furthermore, the color glass condensate calculation can describe the ALICE data up to intermediate-$p_{\rm T}$, and only the MV$^{\gamma}$ parametrization (McLerran-Venugopalan model with anomalous dimension-γ) can describe the ALICE data for large-$p_{\rm T}$ region in ultrarelativistic heavy ion collisions[19]. Indeed, the dileptons and photons were shown to be sensitive probe of the gluon saturation dynamics in relativistic heavy ion collisions since there has no strong interaction with the nuclear medium final state.

In the paper, we investigate the production of dileptons and photons in the CGC approach in ultrarelativistic heavy ion collisions at RHIC energies and Large Hadron Collider (LHC) energies. At high energies, the dynamical features of the CGC can be obtained from the Jalilian-Marian, Iancu, McLerran, Weigert, Leonidov and Kovner (JIMWLK) renormalization group equation, which describes the statistical weight function $W[\rho_{\rm c}]$ for a given Bjorken x, where $\rho_{\rm c}$ is the color source[7–12]. In the infinite momentum

Received date: 19 May 2015; **Revised date:** 18 Jun. 2015

Foundation item: National Natural Science Foundation of China (11465021, 11065010)

Biography: YU Gongming (1985–), male (Bouyei Nationality), Kunming, Yunnan, China, postgraduate, working on the field of Quark-Gluon plasma; E-mail: ygmanan@163.com.

Corresponding author: LI Yunde, E-mail: yndxlyd@163.com.

frame, the saturated gluon distribution $W[\rho_{\rm c}]$ carries much more information than the parton distribution functions(PDF). Furthermore, the saturation scale increases with energy $Q_{\rm s}^2 \sim (x_0/x)^{\lambda}$, where x is the fraction of energy for a gluon and λ is the saturation exponent[20–22]. Indeed, the saturation momentum at LHC energies will become larger than the QCD confinement scale $\Lambda_{\rm QCD}$ in ultrarelativistic heavy ion collisions that can separate the CGC physics from the nonperturbative effects since the running coupling constant $\alpha_{\rm s} \ll 1$[20–22]. Based on the $k_{\rm T}$-factorization approach, we consider the dileptons and direct photons produced by the gluon-gluon interaction in the CGC. Since high energy nucleus-nucleus interactions are determined by gluon partons, we have to insert a quark loop into a gluon ladder for a virtual photon which splits into a dilepton. For photons production, we also have to insert a quark loop into a gluon ladder for $x \ll 1$ since gluon carry no charge.

This paper is organized as follows. In Sec. 2, we present the production for dileptons and photons from the color glass condensate based on the $k_{\rm T}$-factorization approach in relativistic nucleus-nucleus collisions. Finally, the conclusion is given in Sec. 3.

2 General formalism

In the CGC approach, the running coupling constant $\alpha_{\rm s}(p_{\rm T})$ replaced by $\alpha_{\rm s}(Q_{\rm s})$, where $p_{\rm T}$ is the transverse momentum of the gluon jet and $Q_{\rm s}$ is the saturation scale in the hadron. The running of the Quantum Chromodynamics coupling is a higher order effect, the one-loop-like running can be written as

$$\alpha_{\rm s}(Q_{\rm s}) = \frac{4\pi}{\beta_0 \ln(Q_{\rm s}^2/\Lambda_{\rm QCD}^2)} \ , \tag{1}$$

where $\beta_0 = 11 - \frac{2}{3}N_f$, and $Q_{\rm s}$ is the saturation scale.

At high energies, the saturation momentum increasing with energy is considered as a free parameter which will cut off uncertainties from fitting electron-proton cross section data and the modeling of saturation momentum. The saturation scale form for the proton was postulated in the form[23]

$$Q_{\rm s,p}^2(x) = Q_0^2(\frac{x_0}{x})^{\lambda} \ , \tag{2}$$

where $Q_0^2 = 1$ GeV^2, and the parameters $x_0 = 3\times10^{-4}$ and $\lambda = 0.288$ were determined from a fit to the electron-proton deep inelastic scattering (DIS) data at small x. For the nucleus, the saturation momentum scale for the x dependence is given by[23]

$$\begin{aligned} Q_{{\rm s},A}^2(x) &= 0.26A^{1/3}Q_{\rm s,p}(x) \\ &= 0.26A^{1/3}Q_0^2(\frac{x_0}{x})^{\lambda} \ , \end{aligned} \tag{3}$$

where A is the nucleon number. At RHIC and LHC energies, the value of saturation momentum becomes large, namely $Q_{\rm s,p}^2 \approx 0.6$ GeV^2 for p-p collisions and $Q_{{\rm s},A}^2 \approx 2.0$ GeV^2 for Au-Au collisons at RHIC energies, and $Q_{\rm s,p}^2 \approx 1$ GeV^2 for p-p collisions and $Q_{{\rm s},A}^2 \approx 2.6 \sim 4.0$ GeV^2 for Pb-Pb collisions at LHC energies, which implies that $\alpha_{\rm s} \ll 1$. In this kinematical region, the saturation scale can be treated as the hard momentum scale and the dileptons and photons production could be calculated in the perturbative approach.

In the $k_{\rm T}$-factorization approach[24], we have to insert a quark loop into a gluon ladder for a virtual photon which splits into a dilepton. The inclusive cross section for dileptons production in the CGC can be written as

$$\begin{aligned} &\frac{{\rm d}\sigma^{-\ell^+\ell^-}}{{\rm d}M^2{\rm d}^2p_{\rm T}{\rm d}y} = \frac{\alpha^2\alpha_{\rm s}^2C_{\rm F}}{9M^4\pi^6}\sum_{f=1}^{N_f}{\rm e}_f^2\int{\rm d}k_{\rm T}^2\varphi_{\rm g}(x_1,k_{\rm T}^2)\times \\ &\varphi_{\rm g}(x_2,(p-k)_{\rm T}^2)J[F(\kappa_1')]J[F(\kappa_2')]T_{\rm F}(M^2,p_{\rm T}^2) \ , \end{aligned} \tag{4}$$

where M is the invariant mass of the dileptons, $x_{1,2} = (2\sqrt{p_{\rm T}^2+M^2}/\sqrt{s})\exp(\pm y)$, $J[F(\kappa_1')] \approx J[F(\kappa_2')] \approx 14$, and $C_{\rm F} = (N_{\rm c}^2-1)/N_{\rm c}$ is the $SU(N_{\rm c})$ color Casimir operator.

The function $T_{\rm F}(M^2,p_{\rm T}^2)$ is given by[24]

$$T_{\rm F}(M^2,p_{\rm T}^2) = \exp[-\frac{\alpha_s}{3\pi}\ln^2(M^2/p_{\rm T}^2)] \ , \tag{5}$$

where $p_{\rm T}$ is the transverse momentum.

The unintegrated gluon distribution functions is related to the gluon structure functions by

$$xG(x,p_{\rm T}^2) = \int^{p_{\rm T}^2}{\rm d}k_{\rm T}^2\varphi_{\rm g}(x,k_{\rm T}^2) \ , \tag{6}$$

where $\varphi_{\rm g}(x,k_{\rm T}^2)$ is the unintegrated gluon distribution functions which describes the probability of finding a gluon with the x fraction of energy and $k_{\rm T}$ transverse momentum.

In the saturation region, we take a simplified form of the gluon density, namely[25]

$$xG(x,p_{\rm T}^2) = \begin{cases} \dfrac{\kappa}{\alpha_{\rm s}}Sp_{\rm T}^2(1-x)^4, & p_{\rm T} < Q_{\rm s}(x) \ , \\ \dfrac{\kappa}{\alpha_{\rm s}}SQ_{\rm s}^2(x)(1-x)^4, & p_{\rm T} > Q_{\rm s}(x) \ , \end{cases} \tag{7}$$

where $Q_{\rm s}^2(x)$ is the gluon saturation scale, the normalization coefficient κ has been determined from the

RHIC data, the factor $(1-x)^4$ is introduced to describe the fact that the gluon density is small at $x \to 1$ as described by the quark counting rules.

In the CGC gluon saturation framework, we also have to insert a quark loop into a gluon ladder for $x \ll 1$ in the $k_{\rm T}$-factorization approach since gluon carry no charge[24]. The invariant cross section of direct photons produced in the relativistic nucleus-nucleus collisions from the CGC is given by

$$\frac{{\rm d}\sigma^{-\gamma}}{{\rm d}^2 p_{\rm T}{\rm d}y} = \frac{\alpha\alpha_{\rm s}^2 C_{\rm F}}{4\pi^2}\sum_{f=1}^{N_f} e_f^2 \frac{1}{F_1(\kappa')}\frac{1}{F_2(\kappa')}\frac{1}{p_{\rm T}^2}\times \int {\rm d}k_{\rm T}^2 \varphi_{\rm g}(x_1, k_{\rm T}^2)\varphi_g(x_2, (p-k)_{\rm T}^2)\ , \tag{8}$$

where $x = (p_{\rm T}/\sqrt{s})\exp(\pm y)$, and the function $F(\kappa')$ can be written as[24]

$$F(\kappa') = -f(\kappa') + 2\kappa'\frac{{\rm d}f(\kappa')}{{\rm d}\kappa'} + 1\ , \tag{9}$$

with

$$f(\kappa') = \begin{cases} \sqrt{\kappa'(1-0.21\ln\kappa')}, & \kappa' \leqslant 1\ , \\ 1, & \kappa' > 1\ , \end{cases} \tag{10}$$

and the variable κ' is given by

$$\kappa'_{1,2} = \frac{12.7\ln[\sqrt{s}/p_{\rm T} \pm y]}{\ln^2(p_{\rm T}^2/\Lambda_{\rm QCD}^2)}\ , \tag{11}$$

here $\sqrt{s}$ is the center-of-mass energy.

The numerical results of dileptons and photons production in the CGC approach at RHIC and LHC energies are plotted in Figs. $1 \sim 3$. In the Figs. 1 and 2 we plot the cross section of dilepton production in the color glass condensate for different mass bins: $0.1 < M < 0.2$ GeV, $0.2 < M < 0.3$ GeV, $0.3 < M < 0.5$ GeV, $0.5 < M < 0.75$ GeV, and $0.75 < M < 1$ GeV. It shows that the CGC makes a good description of low-$p_{\rm T}$ dileptons production. The parton mass affects the gluon evolution towards saturation, therefore the saturation exponent $\lambda = 0.288$ is reduced from the RHIC data. In this state, the parton density with transverse momentum less than the saturation momentum $Q_{\rm s}$ will reach a high value. This leads to the contribution for low-$p_{\rm T}$ dileptons production from the CGC is evident for p-p collisions ($\sqrt{s} = 200$ GeV, $\sqrt{s} = 7$ TeV and $\sqrt{s} = 14$ eV), for Au-Au collisions ($\sqrt{s} = 200$ GeV), for p-Pb collisions ($\sqrt{s} = 5.02$ TeV), and for Pb-Pb collisions ($\sqrt{s} = 2.76$ ATeV and $\sqrt{s} = 5.5$ ATeV) in ultrarelativistic heavy ion collisions. In Fig. 3 we plot the cross section of low-$p_{\rm T}$ direct photons production from the CGC. The peak of the $p_{\rm T}$ distribution of the invariant cross-section for direct photons is further enhanced by saturation effects. The numerical results show that the contribution for direct photons produced by the gluon-gluon interaction is prominent for p-p collisions ($\sqrt{s} = 200$ GeV, $\sqrt{s} = 7$ TeV and $\sqrt{s} = 14$ TeV), for Au-Au collisions ($\sqrt{s} = 200$ GeV), for p-Pb collisions ($\sqrt{s} = 5.02$ TeV), and for Pb-Pb collisions ($\sqrt{s} = 2.76$ ATeV and $\sqrt{s} = 5.5$ ATeV) in ultrarelativistic heavy ion collisions.

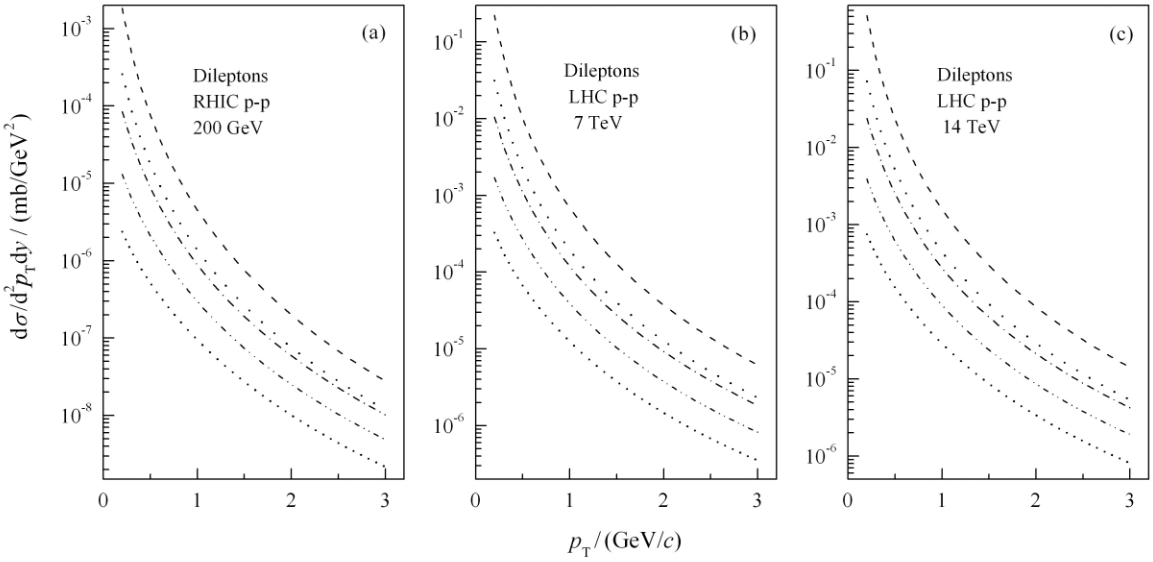

Fig. 1　The invariant cross section of dileptons production from the CGC for p-p collisions at RHIC energies and LHC energies. The dash line: $0.1 < M < 0.2$ GeV; the dot line: $0.2 < M < 0.3$ GeV; the dash-dot line: $0.3 < M < 0.5$ GeV; the dash-dot-dot line: $0.5 < M < 0.75$ GeV; the short-dash line: $0.75 < M < 1$ GeV.

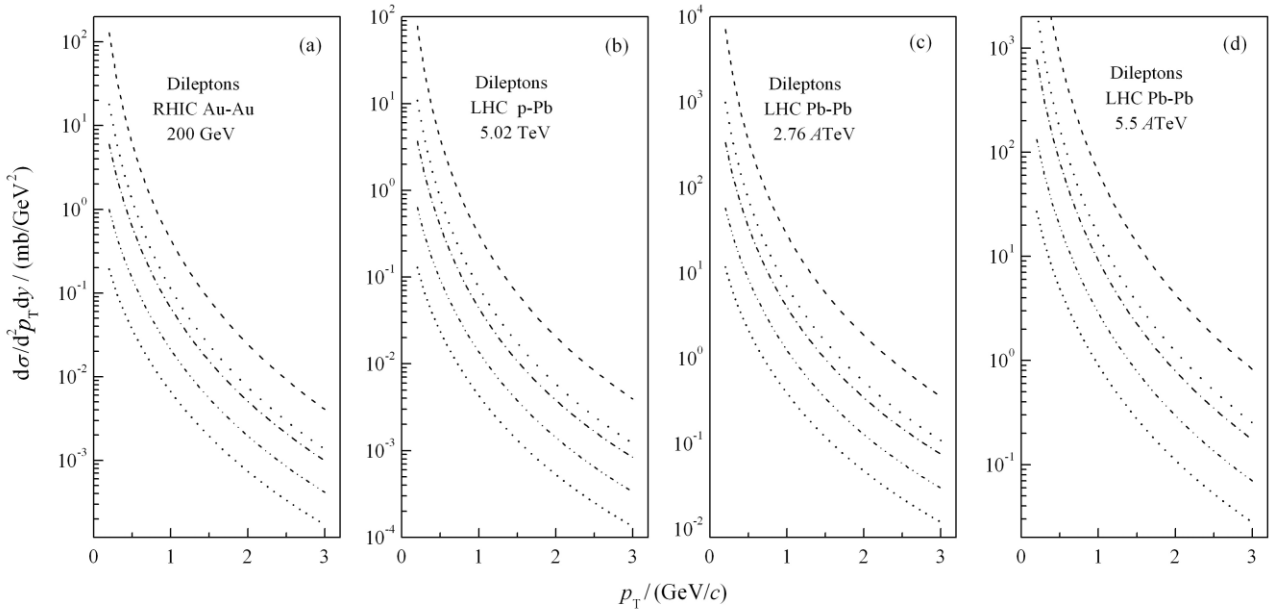

Fig. 2 The invariant cross section of dileptons production from the CGC for Au-Au collisions at RHIC energies, and for p-Pb collisions and Pb-Pb collisions at LHC energies. The dash line: $0.1 < M < 0.2$ GeV; the dot line: $0.2 < M < 0.3$ GeV; the dash-dot line: $0.3 < M < 0.5$ GeV; the dash-dot-dot line: $0.5 < M < 0.75$ GeV; the short-dash line: $0.75 < M < 1$ GeV.

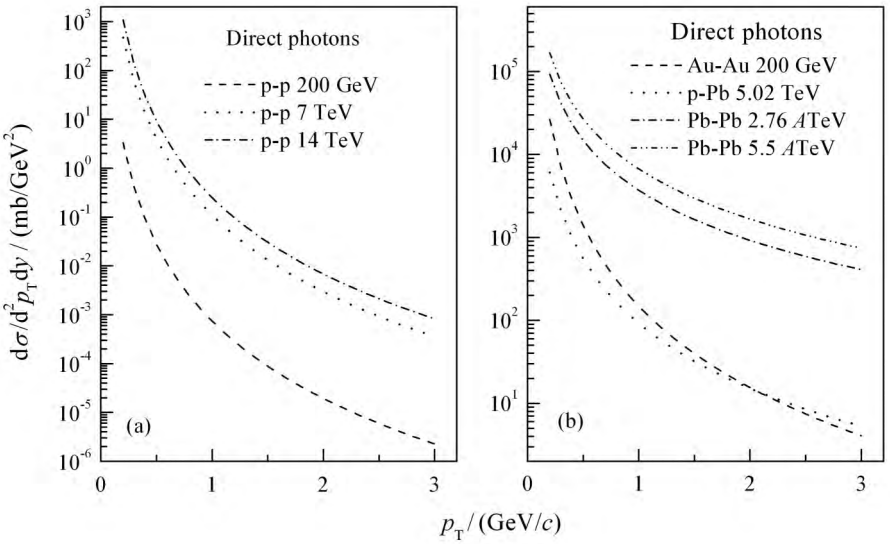

Fig. 3 The invariant cross section of direct photons production from the CGC in ultrarelativistic heavy ion collisions at RHIC and LHC energies.
(a) The dash line for p-p collisions with $\sqrt{s} = 200$ GeV, the dash line for p-p collisions with $\sqrt{s} = 7.0$ TeV, the dash-dot line for p-p collisions with $\sqrt{s} = 14.0$ TeV. (b) The dash line for Au-Au collisions with $\sqrt{s} = 200$ GeV, the dot line for p-Pb collisions with $\sqrt{s} = 5.02$ TeV, the dash-dot line for Pb-Pb collisions with $\sqrt{s} = 2.76$ TeV, the dash-dot-dot line for Pb-Pb collisions with $\sqrt{s} = 5.5$ TeV.

3 Summary

In summary, We have investigated the low-p_{T} dileptons and direct photons production in the k_{T}-factorization approach from the CGC. In the CGC gluon saturation framework, the dileptons and direct photons are mainly produced by the gluon-gluon interaction. Since gluon carry no charge, we have to insert a quark loop into a gluon ladder for dileptons and direct photons production in the CGC. The CGC makes a good description of low-p_{T} dileptons and direct photons production. The value of saturation momentum at high energies becomes larger than the QCD confinement scale for relativistic heavy ion collisions,

which implies that $\alpha_s \ll 1$. The saturation exponent at LHC energy is smaller than that at RHIC energy due to mass effect slowing down the gluon evolution towards saturation. In this state, the parton density with transverse momentum less than the saturation momentum Q_s will reach a high value. The numerical results show that the contribution of low-p_T dileptons and direct photons produced by gluon-gluon interaction from the CGC becomes evident for p-p collisions ($\sqrt{s}=200$ GeV, $\sqrt{s}=7$ TeV and $\sqrt{s}=14$ TeV), for Au-Au collisions ($\sqrt{s}=200$ GeV), for p-Pb collisions ($\sqrt{s}=5.02$ TeV), and for Pb-Pb collisions ($\sqrt{s}=2.76$ ATeV and $\sqrt{s}=5.5$ ATeV) in ultrarelativistic heavy ion collisions.

References:

[1] GELIS F, IANCU E, JALILIAN-MARIAN J, VENUGOPALAN R. Ann Rev Nucl Part Sci, 2010, **60**: 463.
[2] ALTARELLI G, PARISI G. Nucl Phys B, 1977, **126**: 298.
[3] DOKSHITZER Y L, DIAKONOV D, TROIAN S I. Phys Rep, 1980, **58**: 269.
[4] DNMITRU A, HAYASHIGAKI A, JALILIAN-MARIAN J. Nucl Phys A, 2006, **765**: 464.
[5] BALIASKY I. Nucl Phys B, 1996, **463**: 99.
[6] KOVCHEGOV Y. Phys Rev D, 2000, **60**: 034008.
[7] JALILIAN-MARIAN J, KOVNER A, LEONIDOV A, WEIGERT H. Phys Rev D, 1999, **59**: 014014.
[8] JALILIAN-MARIAN J, KOVNER A, LEONIDOV A, WEIGERT H. Nucl Phys B, 1997, **504**: 415.
[9] IACCU E, LEONUDOV A, MCLERRAN L D. Phys Lett B, 2001, **510**: 133.
[10] IACCU E, LEONUDOV A, MCLERRAN L D. Nucl Phys A, 2001, **692**: 583.
[11] WEIGERT H. Nucl Phys A, 2002, **703**: 823.
[12] KOVNER A, MILHANO J, WEIGERT H. Phys Rev D, 2000, **62**: 114005.
[13] IANCU E, MUELLER A H. Nucl Phys A, 2004, **730**: 460.
[14] IANCU E, MUELLER A H. Nucl Phys A, 2004, **730**: 494.
[15] KOZLOV M, LEVIN E. Nucl Phys A, 2004, **739**: 291.
[16] MCLERRAN L, VENUGOPALAN R. Phys Rev D, 1994, **49**: 2233.
[17] MCLERRAN L, VENUGOPALAN R. Phys Rev D, 1994, **49**: 3352.
[18] MCLERRAN L, VENUGOPALAN R. Phys Rev D, 1994, **50**: 2225.
[19] LAPPI T, MNTYSAARI H. Phys Rev D, 2012, **88**: 114020.
[20] XIANG W C, ZHANG J J, ZHOU D C, CHEN S G, LIU W S. Chin Phys Lett, 2013, **30**: 062501.
[21] XIANG W C, ZHANG J J, CHEN S G, LIU W S, ZHOU D C. Chin Phys Lett, 2013, **20**: 082501.
[22] HU J B, SHANG L B, SONG X S, CHEN S G, ZHOU D C, XIANG W C. Chin Phys Lett, 2014, **31**: 032501.
[23] KOWALSKI H, LAPPI T, VENUGOPALAN R. Phys Rev Lett, 2008, **100**: 022303.
[24] GRIBOV L V, LEVIN E M, RYSKIN M G. Phys Rep, 1983, **100**: 1.
[25] KHARZEEV D, LEVIN E, NARDI M. Nucl Phys A, 2005, **747**: 609.

色玻璃凝聚近似下极端相对论重离子碰撞中的双轻子和光子产生

余功明[1]，杨海涛[2]，李云德[1]

（1. 云南大学物理系，昆明　650091；
2. 昭通学院物理与电子信息工程学院，云南 昭通　657000）

摘要： 在色玻璃凝聚胶子饱和框架下，研究了相对论重离子碰撞中的双轻子和光子产生。在胶子饱和区域，在微扰近似 (k_T-因子化近似) 下低转移动量双轻子和光子的主要产生机制是胶子-胶子相互作用。在 RHIC 和 LHC 能量区域的相对论重离子碰撞中，饱和动量的值远远大于量子色动力学禁闭标度 Λ_{QCD}，这使得$\alpha_s \ll 1$。此时，当转移动量小于饱和动量Q_s时质子和原子核的胶子密度值就会很高，双轻子和光子的不变产生横截面会由于饱和效应而得到增强。数值结果给出在 RHIC 和 LHC 能量区域的 pp, pA 和 AA 碰撞中，来源于色玻璃凝聚的低转移动量双轻子和光子产生贡献是显著的。

关键词： 双轻子；光子；色玻璃凝聚；重离子碰撞

收稿日期： 2015-05-19；　**修改日期：** 2015-06-18

基金项目： 国家自然科学基金资助项目(11465021, 11065010)

通信作者： 李云德，E-mail：yndxlyd@163.com。